IN VITRO ELECTROCHEMICAL EVALUATION OF BIOELECTRONIC PROBES

Sukhpreet Singh

Thesis Prepared for the Degree of

MASTER OF SCIENCE

UNIVERSITY OF NORTH TEXAS

December 2021

APPROVED:

Melanie Ecker, Committee Chair
Xiaodan Shi, Committee Member
Vijay Vaidyanathan, Committee Member and Chair of the Department of Biomedical Engineering
Hanchen Huang, Dean of the College of Engineering
Victor Prybutok, Dean of the Toulouse Graduate School

Singh, Sukhpreet. *In Vitro Electrochemical Evaluation of Bioelectronic Probes*. Master of Science (Biomedical Engineering), December 2021, 45 pp., 7 tables, 15 figures, 3 appendices, 25 numbered references.

In this paper, I sought to identify and develop a protocol on electrode arrays as a result of rapid aging by applying rapid current over time. We, however, apply a different approach by using phosphate buffer solution (PBS) to mimic the conditions of the body. Here we have established an in vitro protocol for accelerated aging, a process that involves testing in extreme conditions such as oxygen, heat, sunlight, humidity, and vibration aimed at speeding the normal aging process of items; on commercially available shape memory polymer electrode arrays from Qualia over a period of 30 days in PBS. Two electrode arrays were placed in 37°C and 2 were placed in 57°C. Open lead electrochemical impedance spectroscopy (EIS) was conducted on the electrode arrays. Overall, the results showed there were differences in average impedance during this accelerated aging protocol. At 37°C we see that the average impedance values increased as the electrodes were aged at 1kHz from an average of 4.15E6 to 9.14E6 Ohms. At 57°C electrode arrays 4 and 5 showed strong P values well above 0.05, but average impedance increased drastically from 3.27E6 to 9.97E6 and P value of 0.04 from measurement day 24 to day 30. This indicated to us that the electrode could be experiencing some delamination. In addition, this could be because the Qualia nerve cuffs tested were "B" grade, so changes in impedance could be due to the integrity of the device. This would tell us that these electrode arrays would not be capable to withstand long – term recording for up to 240 days. As a result, rejecting the hypothesis that this protocol would show no change in impedance levels for a simulated aging period of 240 days. Although this protocol was not in a perfect setting and the quality of the electrodes were not up to standard, this gave us insight into the electrochemical properties of SMP electrodes which will be useful when we bio-fabricate our own electrodes to study gastrointestinal (GI) disorders.

ACKNOWLEDGEMENTS

This research was supported by the University of North Texas Biomedical engineering department and Dr. Melanie Ecker's lab. I would like to thank Dr. Ecker for being very patient with me during this process. She showed me how to set a goal and then execute to obtain the goal. She has taught me how to develop a whole new experiment from the ground up. I am honored to have made a protocol that can eventually be used to help us understand the relationship between ENS dysfunction and GI disorders. I would also like to thank the rest of the academic committee for taking time to be a part of this presentation. I am very thankful and grateful for the experience. This made me into a better student, and I will take this moment and apply it within my future endeavors.

TABLE OF CONTENTS

Page

LIST OF TABLES

Page

LIST OF FIGURES

Page

CHAPTER 1

INTRODUCTION

1.1 Research Overview

In this paper, I sought to identify and develop a protocol on electrode arrays as a result of rapid aging by applying rapid current over time. We presume that the electrodes are capable of withstanding long periods without material compromise. *In vitro* process is essential as it enables testing of electrodes in the development period. Previous similar experiments have used hydrogen peroxide that caused degradation of the electrodes thus, rendering them useless. We, however, apply a different approach by using phosphate buffer solution (PBS) to mimic the conditions of the body. Here we have established an *in vitro* protocol for accelerated aging, a process that involves testing in extreme conditions such as oxygen, heat, sunlight, humidity, and vibration aimed at speeding the normal aging process of items; on commercially available shape memory polymer electrode arrays from Qualia over a period of 30 days in PBS. Two electrode arrays were placed in 37°C and 2 were placed in 57°C. Open lead electrochemical impedance spectroscopy (EIS) was conducted on the electrode arrays. Overall, the results showed there were differences in average impedance during this accelerated aging protocol. At 37°C we see that the average impedance values increased as the electrodes were aged at 1kHz from an average of 4.15E6 to 9.14E6 Ohms. At 57°C electrode arrays 4 and 5 showed strong P values well above 0.05, but average impedance increased drastically from 3.27E6 to 9.97E6 and P value of 0.04 from measurement day 24 to day 30. This indicated to us that the electrode could be experiencing some delamination. In addition, this could be because the Qualia nerve cuffs tested were “B” grade, so changes in impedance could be due to the integrity of the device. This would tell us that these electrode arrays would not be capable to withstand long – term recording for up to 240 days. As

a result, rejecting the hypothesis that this protocol would show no change in impedance levels for a simulated aging period of 240 days. Although this protocol was not in a perfect setting and the quality of the electrodes were not up to standard this gave us insight into the electrochemical properties of SMP electrodes which will be useful when we bio-fabricate our own electrodes to study gastrointestinal (GI) disorders.

1.2 Research Goal

To develop a reproducible protocol that helps us understand whether the electrode arrays are stable for long – term recording. We are hypothesizing that when performing the electrochemical evaluation of the electrodes in 7.4 pH PBS solution, we will see that there are no effects to the performance of the device at normal physiological temperature (37°C). Also, when raising the temperature to more extreme conditions (57°C), we are hopeful to see no change in average impedance values. This will give us a better understanding of these bioelectronic devices, to then apply this protocol for future electrode arrays to study enteric nervous system (ENS) disfunctions correlating to gastrointestinal disorders.

CHAPTER 2

BACKGROUND

Dysfunction of the enteric nervous system (ENS) can be related to several things such as, irritable bowel syndrome, inflammatory bowel disease which includes ulcerative colitis and Crohn's disease. Roughly 10- 15% of the population is affected by irritable bowel syndrome (21). Unfortunately, the technology is not readily available for us to understand the issues behind ENS disfunction correlating to gastro-intestinal (GI) disorders. The ENS embodies a majority of neurons in the peripheral nervous system, but when comparing it to the central nervous system research conducted has been insignificant (22). If we were to gain access to it, then we would be better equipped to understand the dysfunctions relating to the ENS. As a result, improving the quality of lives for the millions that are affected by GI disorders. If ENS disfunction is causal for these disorders, one can envision a bi-directional interface that can perform recording and stimulation as a neuroprosthesis.

Current research over the function and electrophysiology of the ENS has been done ex vivo, either on pathological flat sheet samples or cell culture. Less work has been done to study electrical recordings of the ENS *in vivo*, which would be necessary to understand the relationships between ENS disfunction and GI disorders (24). Examples of the *in vivo* testing include nonantibiotics development, new surgical procedures and the pathogenesis of disease. With any foreign body being surgically implanted there are some things to take into consideration such as biocompatibility, implant size, tissues being affected, and degradation. Specifically, for this research we will establish a protocol to look at the overall electrochemical performance of the 4 – channel Qualia microelectrode array *in vitro* in order to evaluate the recording durability and longevity of the microelectrode. We are still in the process of developing the bioelectronic

devices, however, we would still need an understanding of the aging process of neural implants relating to the ENS. Thus, we are using commercially available devices from Qualia Labs that are comparable to the devices we are developing, to realize the objective of this research. In addition to it being cost effective, this *in vitro* system to accelerate the aging process would allow us to test the bioelectrodes frequently and decrease the development process of the bioelectrodes.

Usually, medical devices are tested by soaking the device in buffer solution coupled with hydrogen peroxide at an elevated temperature to accelerate the aging process (23). The rate of chemical reactions increases exponentially with increasing temperatures according to the Arrhenius law equation

$$k = Ae^{-E} \quad \text{(Eq. 1)}$$

where k is the rate constant, A is the pre – exponential factor, -E is the activation energy, R is the universal gas constant, and T is the temperature. And as a result, using the Arrhenius equation allows us to determine how the accelerated aging time *(R_2)* relates to aging at a desired real time (R_1) for different temperatures (T) (Eq. 2)

$$R_2 = R_1 Q_{10}^{(T_2 - T_1)/10°C} \quad \text{(Eq. 2)}$$

Q_{10} is the aging factor, which is 2 for polymeric substrates according to the ASTM standards F2003-02. Performing the experiment this way would not accurately capture the chemical environment created by active immune cells. These active immune cells release digestive enzymes and reactive oxygen species (ROS). Previous experiments have used hydrogen peroxide coupled with PBS to mimic the effect of reactive oxygen species generation during the brain's injury response. With this protocol, only PBS solution will be used to evaluate the electrochemical performance and longevity of the microelectrode. Previous research conducted

has shown if we place the electrodes in hydrogen peroxide, it causes chemical reaction that will degrade the electrodes faster.

Issues when attaching an electrode to the small intestine, are that the tissue is soft muscle, geometry is irregular, and it is constantly moving. Current electrodes are too stiff and do not conform well enough to provide consistent recordings of the ENS. However, the use of selfsoftening polymers as electrode substrates offers solutions to the problem, therefore giving us the potential to gain insight into GI electrophysiological knowledge in live animals when *in vivo* analysis is eventually conducted.

2.1 Neural Microelectrodes

The purpose of neural electrodes is to allow us to record signals from several neurons, termed action potentials. Performing *in vitro* studies will give us a better understanding between neurons and electrochemical characteristics of the Qualia nerve cuff.

With respect to neurons, there are two factors to consider when evaluating biosensor performance, that is selectivity and sensitivity (7). Selectivity means spatial resolution and sensitivity refers to any absolute changes in potential of a target measurement that can be detected by an instrument. Extracellular and intracellular recordings are among the two measurements that are taken from MEA's. As one can tell from the names, extracellular recordings are taken outside the cell depicting that this method is less invasive and will be more beneficial for long-term studies. Intracellular recordings are invasive, which can lead to cell damage at the placement site (8). In our case, we will be performing all experiments extracellularly *in vitro*. Eventually we will be able to perform the experiments with rodents intracellularly.

2.2 Microelectrode Materials

Advancements in microelectrode arrays have led to the development of different strategies

to improve compatibility. By making the stiff electrode substrates soft with synthetic or biological polymers, lower the electrode impedance and surface hardness of the probes. Thus, glial scarring around the electrode is essentially diminished leaving the electrode unaffected. The idea is to have a lower Young's Modulus to avoid any issues between the electrode and contacting tissue. When selecting insulating materials for the electrode we must keep in mind toxicity, mechanical, and electrical properties.

Microelectrode arrays (MEA's) are favored for *in vivo* studies for recording electrical signals (1). Currently, polymer-based electrodes that have a low Young's modulus are favored (1).

Young's modulus describes the elastic properties of a material undergoing tension or compression in only one direction. This is equal to the longitudinal stress divided by the strain (Eq. 3).

$$E = \frac{\sigma}{\varepsilon} \qquad \text{(Eq. 3)}$$

where E = Young's modulus, pressure units, σ = uniaxial stress, and ε = strain

The materials used for the microelectrode are crucial to ensure that proper elasticity and flexibility are given to address issues dealing with positioning and placement of the electrode. Things such as mechanical strain should be factored in as well. Implantation of stiff electrodes, especially for recording neural signals from the small intestine is not preferable as the small intestine has an irregular shape and is in constant motion. The mechanical strength of the electrodes can affect electrical signals of the electrode from the changes in resistance or capacitance of the material (2).

Traditional microelectrodes are made up of silicone mainly due to the low Young's modulus (1-50 MPa), as well as their stability (3). However, the issue with silicone is that the

material will evoke a negative immune response such as, epineural fibrosis, which restricts nerve stretching. As a result, this affects nerve conduction, which in turn, compromises the electrode. When measuring neural signals, it is also crucial that the electrode is in direct contact with the neurons. The electrodes can either be penetrating or non-penetrating. Additionally, when fabricating the electrodes, we want to be sure that there is no immune response triggered, this could affect the electrode since it must maintain contact with the body for a long period of time (4).

Chronically – implanted electrodes are classified according to its shape and materials of fabrication as shown in Figure 2.1. They can either be single wired, tetrode, or multi wired, respectively (1).

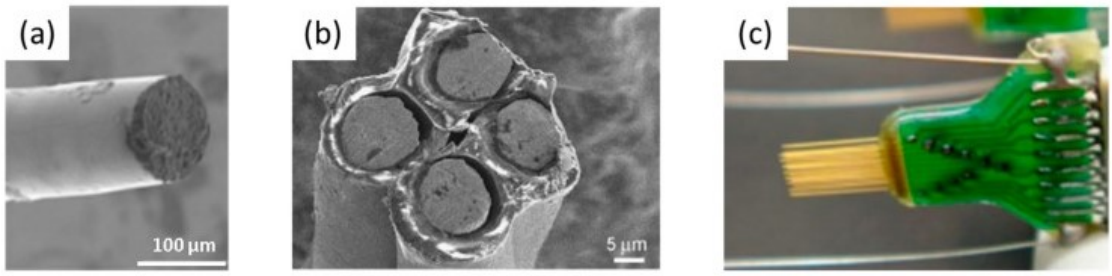

Figure 2.1: The different types of microwire neural electrode. A) single wire, B) Tetrode, C) Multi – wire electrode.

The use of neural interfaces to record action potential signals began in 1968 when Robinson introduced the first microelectrode just before Thomas introduced the first MEA in 1972. (5,6) This array consisting of platinized gold microelectrodes embedded on a glass substrate was only able to measure and record local field potential (LFP) signals, but not activity signals from a single cell.

Silicone based neural electrodes were first introduced in 1970. Dubbed the name "Michigan" electrode, this electrode allowed higher density of sensors for implantation and higher

spatial resolution when compared to microwire MEA's. Wang et al. was able to record action potentials for 671 days with this electrode, demonstrating that it can record for a long period of time (11). In 1990 the "Utah" electrode was developed. Still made up of silicone, this electrode differed from the previous "Michigan" electrode because the silicone needles were vertically placed on the substrate. The downside to this was that the silicone needles were only able to receive signals from the tips of each electrode. As a result, this limited the amount of information that could be obtained from electrode recordings (12). Figure 2.2 depicts both Michigan and Utah electrodes, respectively.

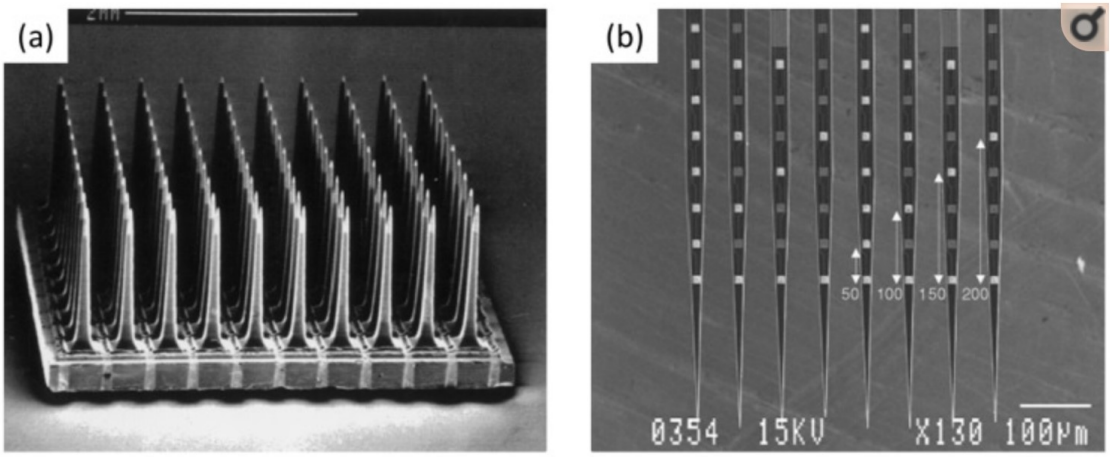

Figure 2.2: (a) Michigan and (b) Utah electrodes

Fabricating electrodes on a stiff material such as silicon has its advantages with respect to overall signal reliability. However, fabricating electrodes on a stiff substrate leads to an inflammatory reaction in which glial scarring occurs because the body is fighting the foreign body (25). The glial scarring will act as an insulator hindering the electrode from functioning properly. To overcome the limitation of stiff substrate materials, polymers have been introduced as a viable substrate for microfabricated probes (13).

Shape memory polymers (SMPs) such as poly (ester urethane) can overcome the challenges during insertion into the tissue like bending because the Young's modulus is decreased significantly from gigapascals to megapascals due to change in temperature or hydration (15). The electrode can remain stiff on the outside to make any necessary adjustments to the electrode surface. Once the electrode is placed inside the body that change in temperature will allow the electrode to conform to the desired surface, in our case that is the small intestine. Shape memory polymers have been introduced with biomedical devices, such as cortical probes. These flexible probes can soften after insertion, making them behave like an elastomer. This concept is demonstrated in Figure 2.3. Although the process in which the shape memory polymer goes from flexible to soft via physiological conditions have not been studied too extensively, it is crucial that we have a clear understanding of the process to fabricate reliable neural electrodes.

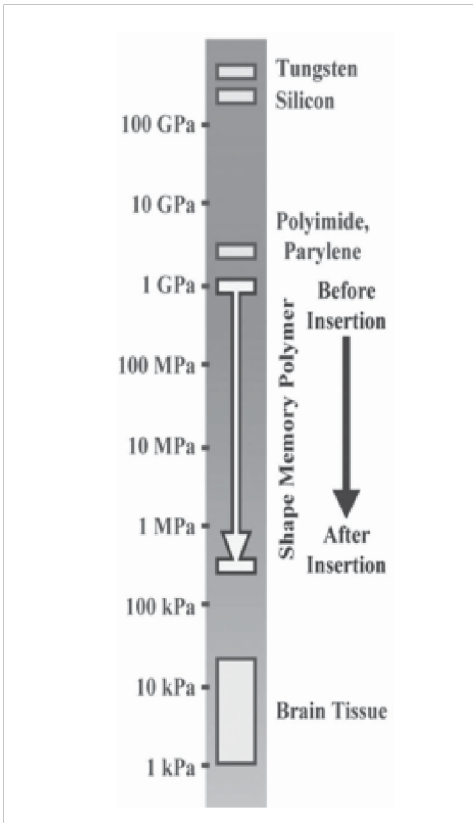

Figure 2.3: **Flexible probes can soften after insertion, making them behave like an elastomer. (15)**

In order to record electrical biopotentials, we need conductive materials for the electrodes and traces. A range of materials have been used for electrodes like tungsten, platinum, iridium oxide, titanium nitride, and poly(ethylenedioxythoiphene) (PEDOT). Research has shown that when electrodes are fabricated with the conducting PEDOT polymer they have the potential to withstand long – term recordings, biocompatibility, and efficient signal, thereby improving overall electrode performance 14).

CHAPTER 3

IN VITRO ELECTROCHEMICAL CHARACTERIZATION

Cyclic voltammetry (CV) and Electrochemical impedance spectroscopy (EIS) are among the common ways we can evaluate the electrochemical performance of electrodes. For the purposes of this protocol we will be focusing on electrochemical impedance spectroscopy.

3.1 Electrochemical Impedance Spectroscopy

Electrochemical impedance spectroscopy (EIS) is a measurement of electrical impedance and phase angle that is obtained with sinusoidal voltage or voltage excitation of the electrode (9). Frequency and magnitude are the parameters for EIS measurements. A linear current – voltage response is evaluated at each frequency because the magnitude of voltage excitation is relatively small. The frequency is usually taken over a broad range during electrochemical evaluation of the electrode (<1 Hz to 10^5 Hz). Typical values for voltage excitation are around 10 mV and normally do not exceed 50 mV in magnitude. This method of measurement is the most meaningful when it comes to evaluating the electrodes recording capabilities, along with tissue and electrode properties. An AC voltage of 10 mV was applied over a range of frequencies between 100 kHz – 1 Hz to each electrode channel during EIS testing and the results were recorded in the form of a bode plot. Advantages to bode plots are that frequency is explicit and small impedances in presence of large impedances can be identified easily. The electrochemical cells are modeled as a network of passive electrical circuit elements, called an “equivalent circuit”. There is a double layer capacitance, electron transfer resistance, and uncompensated electrolyte resistance creating a simplified Randle’s cell (Fig. 3.1), which is considered to be the basic unit for EIS. All systems using EIS has this type of circuit. Whether or not everything can be seen/involved within our system is dependent on the electrode and experimental setup. In our simplified Randle’s cell we

have 3 components in the circuit. Cd is the double layer capacitance, Ru is the uncompensated electrolyte resistance, and Rp is the electron transfer resistance. At high frequency the capacitor is not involved within the circuit and all the current is traveling across Cd to Ru and none is going to Rp with a phase shift of 0 degrees. As the frequency is decreasing, the capacitor becomes more involved and that is depicted as the impedance is rising with the phase angle going to 90 degrees. There is a point in which the impedance is too great for the capacitor, therefore the current is divides and at low frequencies the current is going through only Rp and Ru with the phase angle going to 0 degrees. More details of the EIS parameters can be found in the appendix. The initial data collected was used as the baseline measurements for the experiment.

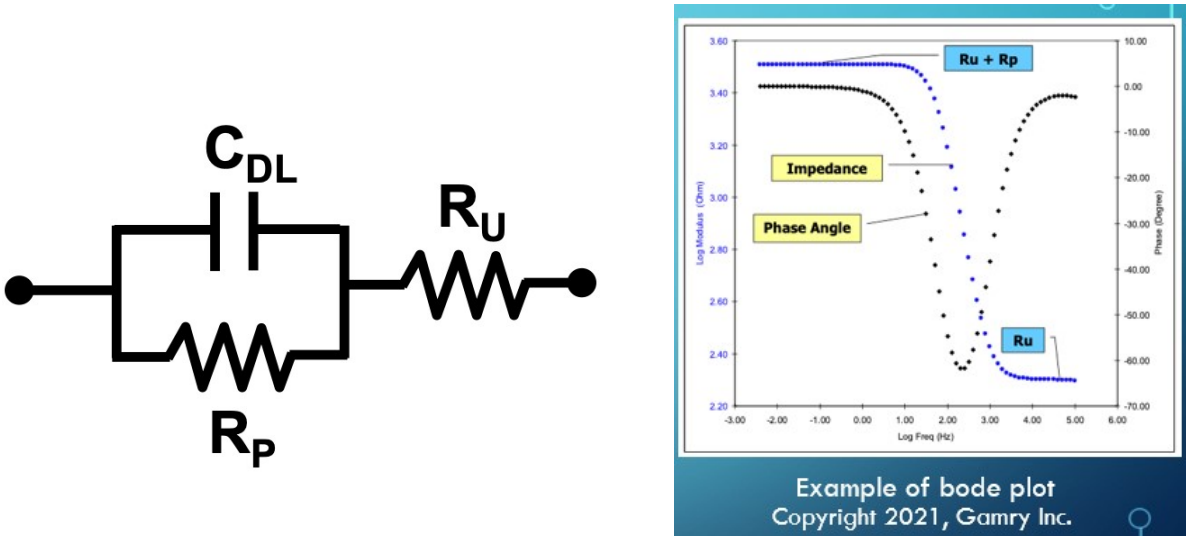

Figure 3.1: Simplified Randle's cell

EIS is critical for bioelectronic devices because it will show us how robust these electrodes are and whether or not they can withstand long – term recording. In addition, this will also tell us if the impedance at 1 kHz is in a sufficient range to record biopotentials with a good signal to noise ratio. Researchers have routinely used 1 kHz to characterize the electrode performance for physiological recording. 1 kHz frequency matches the neural action potential, which is approximately 1 ms long (26).

3.2 Implant Design and Methods and Materials

In this study, four cuff electrodes from Qualia Labs Inc. were used. These electrodes were used to establish protocols for electrochemical functionality and performance under accelerated *in vitro* conditions. These electrode arrays are designed for in vivo animal studies, specifically to study the peripheral nervous system. However, we are primarily interested to use them to getting a better understanding of the electrochemical characteristics of the electrodes. These 4 – channel electrodes were fabricated using traditional photolithography techniques with titanium nitride as the electrode material to increase the capacitive charge – injection and storage capacity (16). Each channel on the electrode is evenly spaced every 1mm making the device width 4mm. Figure 3.2 shows a picture of the Qualia nerve cuff along with the specs of the device.

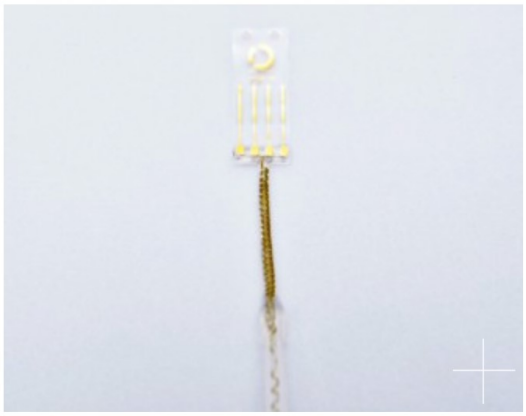

Device length	10.000 mm
Device width	4.000 mm
Device thickness	30 ± 5 µm
Electrode length	1.210 mm
Electrode width	0.150 mm
Electrode area	0.182 mm^2
Electrode sites	4
Electrode spacing	1.000 mm

Figure 3.2: **Qualia nerve cuff and specifications**

3.3 Titanium Nitride (TiN)

The electrodes from Qualia Labs Inc. were fabricated from a metallic compound, titanium nitride. This chemical compound is considered a stable conductor that has shown promising biocompatibility. Titanium nitride exhibits optimal conditions with respect to charge injection

capacities. Previous research has shown that using a large surface area sputtered titanium electrode produces a porous electrode with an in vitro charge – injection capacity of 0.9mC cm-2 for 4000 um^2 (17). This may be less than the charge – injection capacity of other electrode coatings such as iridium oxide, but a high electrode surface area (ESA) to geometric surface area (GSA) ratio could offer higher charge injection capacities. Figure 3.3 shows a scanning electron micrograph of a porous sputtered titanium nitride electrode surface that has a high ESA/GSA ratio. Capacitive charging can involve a double – layer ion – electron charge separation, making it electrostatic. It could also be electrolytic in which charge is stored across a thin, high – dielectric – constant oxide at the electrode – electrolyte interface. Capacitive charge – injection is favorable when compared to faradaic charge – injection, because with faradaic charge- injection, there is an electrochemical reaction in which chemical species are either oxidized or reduced (15). We do not want that happening because when it does come time to implant the electrodes into rodents, the negative foreign body response would degrade the electrode hindering us from getting long – term consistent recordings.

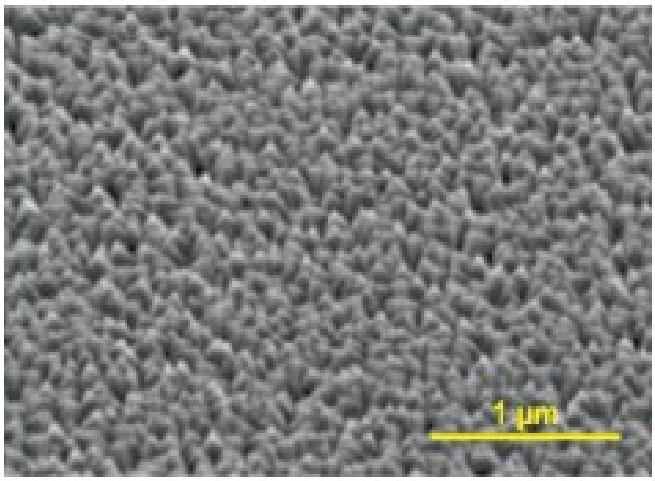

Figure 3.3: Shows a scanning electron micrograph of a porous sputtered titanium nitride electrode surface that has a high ESA/GSA ratio.

CHAPTER 4

EXPERIMENTAL PROCEDURE

4.1 Electrochemical Device Characterization

To evaluate the electrochemical properties of the electrodes electrochemical impedance spectroscopy (EIS) was conducted *in vitro* using Gamry Potentiostat paired with a multichannel multiplexer (Fig. 4.1A). With this instrument we can capture the electrochemical reactions that occur on each individual channel. More specifically this technique allows the characterization of membranes in working conditions without destruction. A three-electrode set up was used for the study (Fig. 4.1B and C), which comprised of one Qualia working electrode (one electrode of the four-channel device), platinum wire as the counter electrode (attached to red alligator clip), and an Ag/AgCl reference electrode.

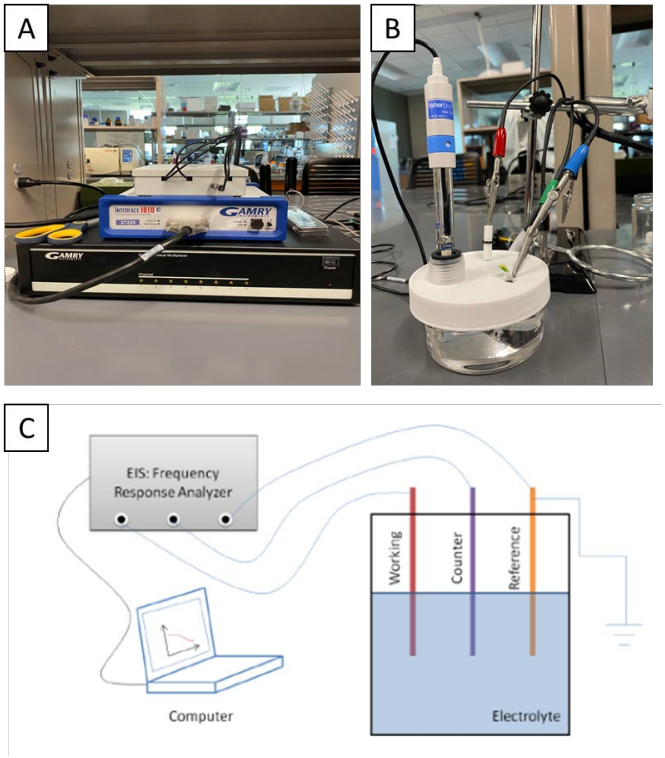

Figure 4.1: Experimental setup for electrochemical characterization. Gamry potentiated used (A), and actual photograph of electrode setup (B), and schematic of wiring (C).

A glass beaker is used to house the phosphate saline solution (PBS) in which the electrode array was submerged in. PBS acts as the electrolyte, mimicking physiological bodily conditions. The reason we are using glass beaker instead of metallic is due to the fact that glass acts as an insulator and that would not interfere with the transfer of electrons during the experimental phase. Alligator clips were then attached to the ends of the electrodes. A working lead (Green) clip were connected to the working electrode. The reference lead (White) was attached to the reference electrode. Then the counter lead is attached to the platinum counter electrode (Red). Within this electrochemical cell the impedance is measured between the reference electrode and the working sense electrode.

This is because the absolute potential of a single electrode cannot be measured therefore, all potential measurements in this EIS systems are performed with respect to a reference electrode (26). Ideally, we would want the working leads to be as far away from the counter and reference leads when performing EIS, but we did not have a faraday cage to keep them separated. All three clips fed into the Gamry which is connected to the computer as shown below. We had a total of 4 devices with four working electrodes each, that were used for the experiment. Each working electrode channel was assigned a number (1-2 & 4-5) and colored tape was attached, blue, yellow, green, and orange respectively. Initial EIS testing without any aging was conducted and the data was used as the baseline measurements.

4.2 Accelerated Aging Studies

To evaluate the durability of the electrode arrays used, we have performed *in vitro* accelerated aging. Each electrode array was suspended in a beaker filled with 7.4 pH PBS solution that mimicked bodily conditions. Four 4 – channel electrode arrays were tested for 30 days. Electrode arrays 1 and 2 are then placed in an incubator at a temperature of 37°C. This mimics

physiological environment. Electrode arrays 4 and 5 are placed in a separate incubator at 57°C for an accelerated aging process. EIS measurements were conducted on arrays 1 and 2 once a week because as hypothesized, the change observed in electrochemical characterization should not be drastic. Arrays 4 and 5 were measured multiple a week because of the elevated temperature. The ASTM International guidelines F2003 – 02 (2008) and F1980-07, suggest using an accelerated aging factor of 2.0 as a conservative estimated value for aging most polymers (20). When the Arrhenius equation (Eq. 2) is applied to this aging scenario, we see that aging under accelerated conditions one day equals four days of aging under normal conditions. Thus, we get a total simulated aging period of 240 days for electrodes 4 and 5 in 57°C after 30 days. Data analysis was then conducted over the results in the form of a bode plot. From there further data analysis was conducted via excel plotting the average impedance values over the aging period in the form of a box plot. We cannot conclude that the electrode arrays showed consistent magnitudes, therefore, a T test was performed to validate that the average impedance values compared stayed within our threshold of 0.05. If the P value was less than 0.05 than we can reject the null hypothesis, but if it is above then we can say that the average impedance values for the tested interval (day 0 to day 7, day 7 to day 14, day 14 to day 21, and day 0 to day 21) are not statistically significant.

CHAPTER 5

RESULTS AND DISCUSSION

In this research study, we established a protocol to rapidly age Qualia microelectrode arrays. In addition, we want to see if the electrodes are robust enough to withstand long periods recording without compromising the material. This *in vitro* process would allow for quicker results and testing the electrodes during the development cycle, as well as providing us a direct comparison between real and simulating aging. Our protocol was tested in two different temperature environments. Two electrode arrays were placed in an incubator set to 37 °C. The other two electrode arrays were placed in slightly harsher conditions at 57 °C, for the same duration. Ideally, we expect reactive oxygen species will not appear during the process. Generation of the ROS would indicate that the channel has been degraded, making the electrode non-viable for future experiments. We used phosphate buffer solution which will mimic bodily condition versus aging them in air. In addition, if the electrodes separate from the cables, then the channel will not be active which can compromise the electrode giving inaccurate readings.

This protocol used open lead EIS, which is useful when dealing with coatings due to their high impedance and small capacitance. This test measures the cable capacitance giving us insight into the limits of the electrode and whether or not we are overloading them. The data looked like a capacitor thus displayed a linear magnitude with 90 degrees of phase angle and when there is resistance the graph should show 0 degrees of phase angle. In addition, the way the alligator clips were connected had an effect on the measurements. The initial measurement is shown in green.

As the frequency decreased the impedance was increasing, but once impedance was above 10 milliohms the electrode experienced overload. That is shown once the magnitude when from linear to being inconsistent and scattered throughout the data. As frequency was decreasing

impedance was increasing linearly with a phase angle going towards 90 degrees, depicting capacitance. Once frequency hit 100 Hz, impedance plateaued with phase angle going to 0 degrees indicating resistance. (Fig. 5.1). The same result was also observed on electrode 2 channel 2. If the excitation is too big then, harmonics are generated when measuring EIS and the data becomes invalid. This is observed on electrode 2 channel 3 (Fig. 5.2).

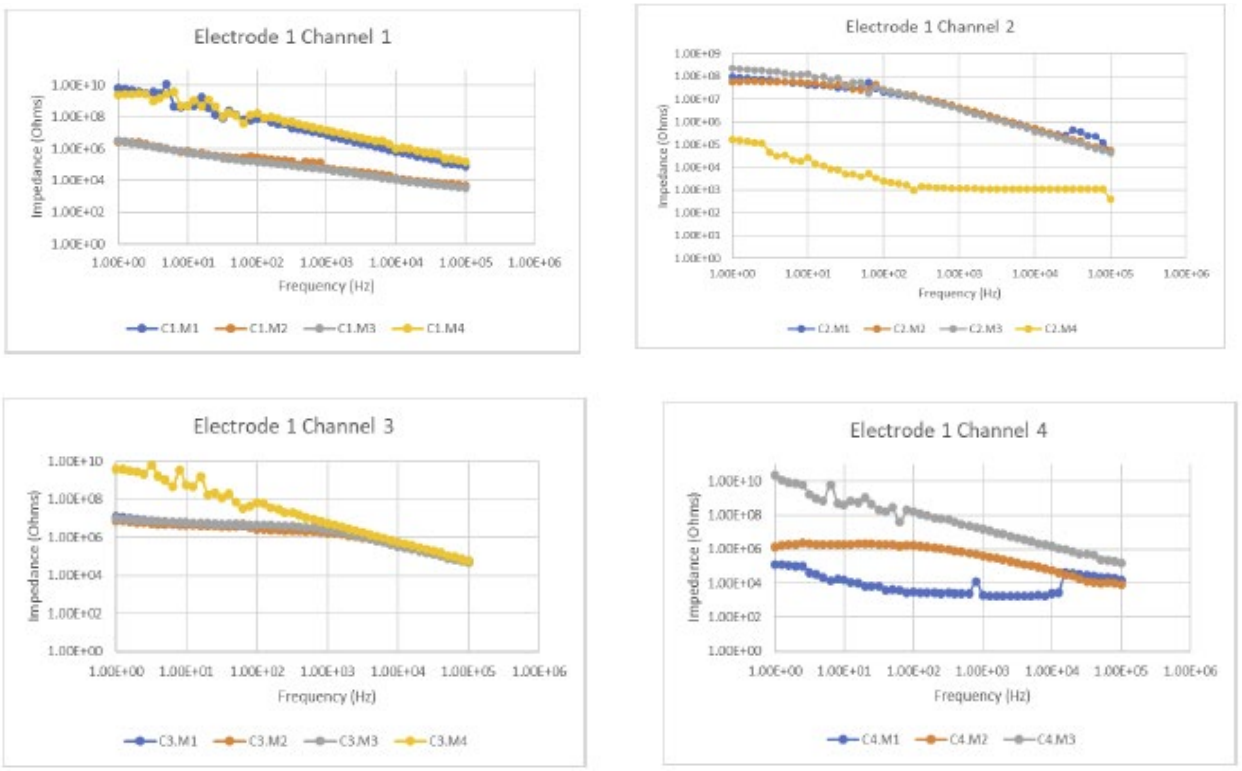

Figure 5.1: Electrode 1

Green = Measurement 1 at 37°C, Blue = Measurement 2 at 37°C, Red = Measurement 3 at 37°C, Purple = Measurement 4 at 37°C X Axis = Frequency (Hz) Y Axis = Impedance (Ohms)

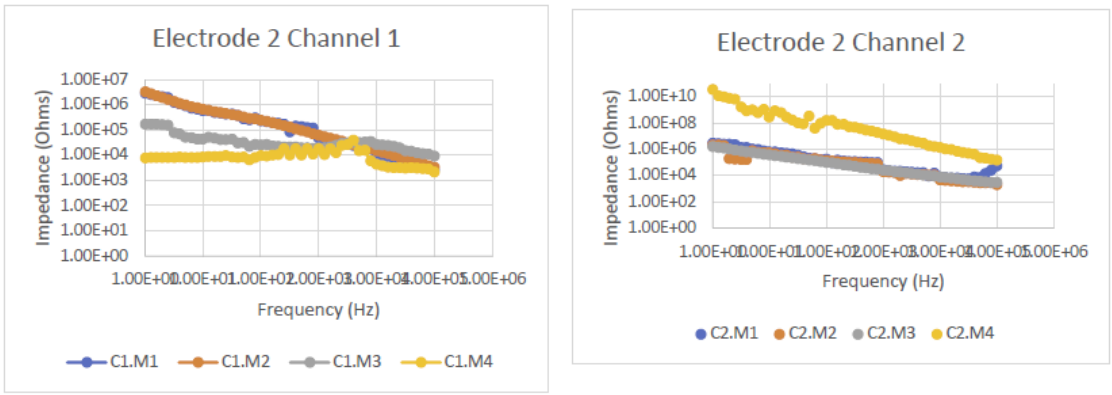

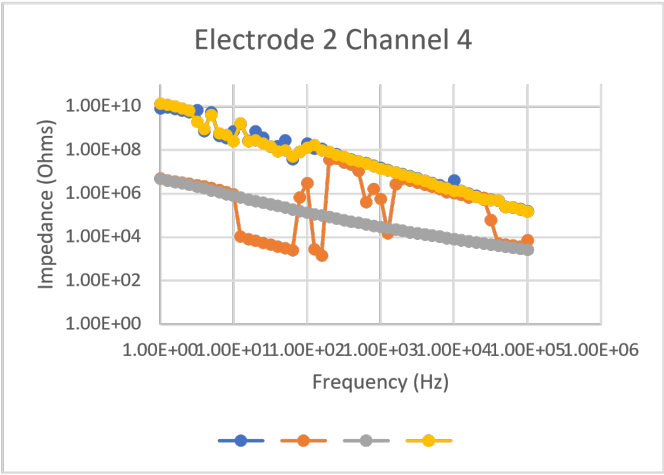

Figure 5.2: Electrode 2

Green = Measurement 1 at 37°C, Blue = Measurement 2 at 37°C, Red = Measurement 3 at 37°C, Purple = Measurement 4 at 37°C X Axis = Frequency (Hz) Y Axis = Impedance (Ohms)

The red line on Channel 3 is an example of when harmonics are observed. The data is scattered and not consistent until the frequency is 10 Hz. This could be from a bad connection to the working electrode. The first two measurements in channel 1 and 2 are consistent with each other, but these were when the set up was 3 lead and not the 4-lead set up. In addition, channel 4 on electrode 2 came off of the electrode leaving that area vulnerable to PBS flowing in causing the electrode to malfunction.

When looking at electrodes 4 and 5 which were aged in 57 °C the overall results were similar to that of electrodes 1 and 2 which were placed in 37 °C (see Figs. 5.3 and 5.4). Electrode 4 channel 1 had 2 measurements that experienced very high impedance at low frequency.

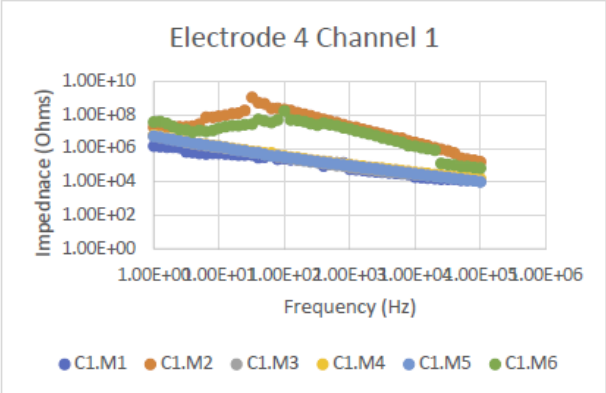

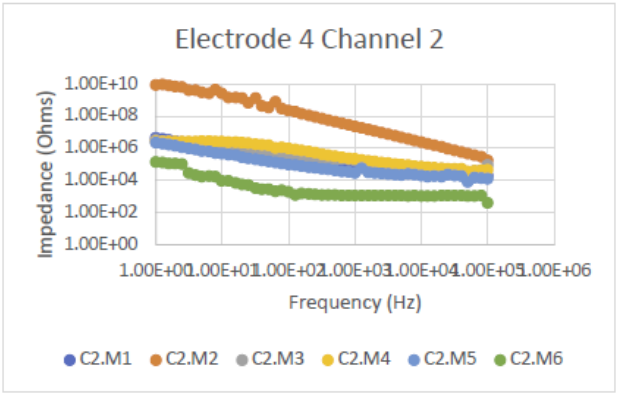

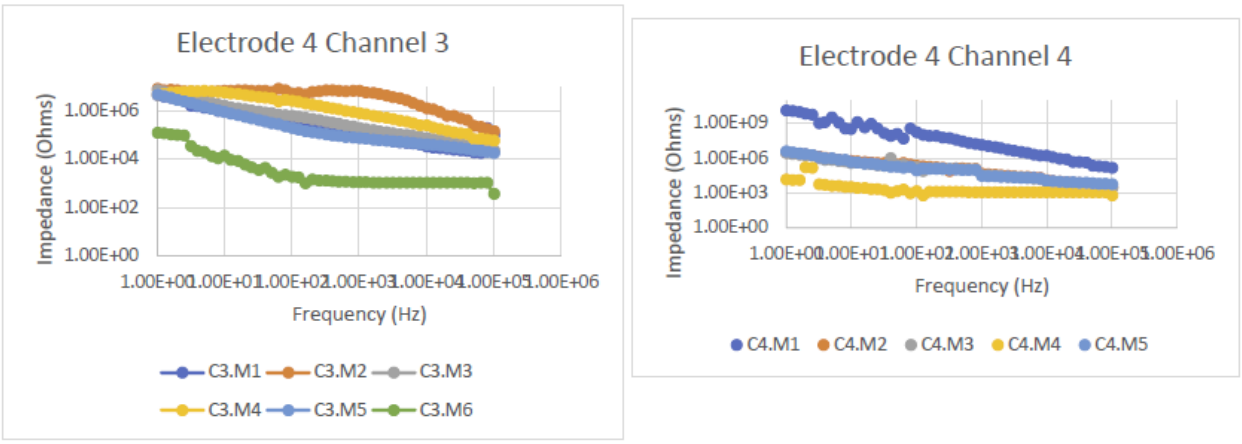

Figure 5.3: Electrode 4

Gray = Measurement 1 at 57°C, Blue = Measurement 2 at 37°C, Red = Measurement 3 at 57°C, Purple = Measurement 4 at 57°C Green = Measurement 5 at 57°C, Brown = Measurement 6 at 57°C X Axis = Frequency (Hz) Y Axis = Impedance (Ohms)

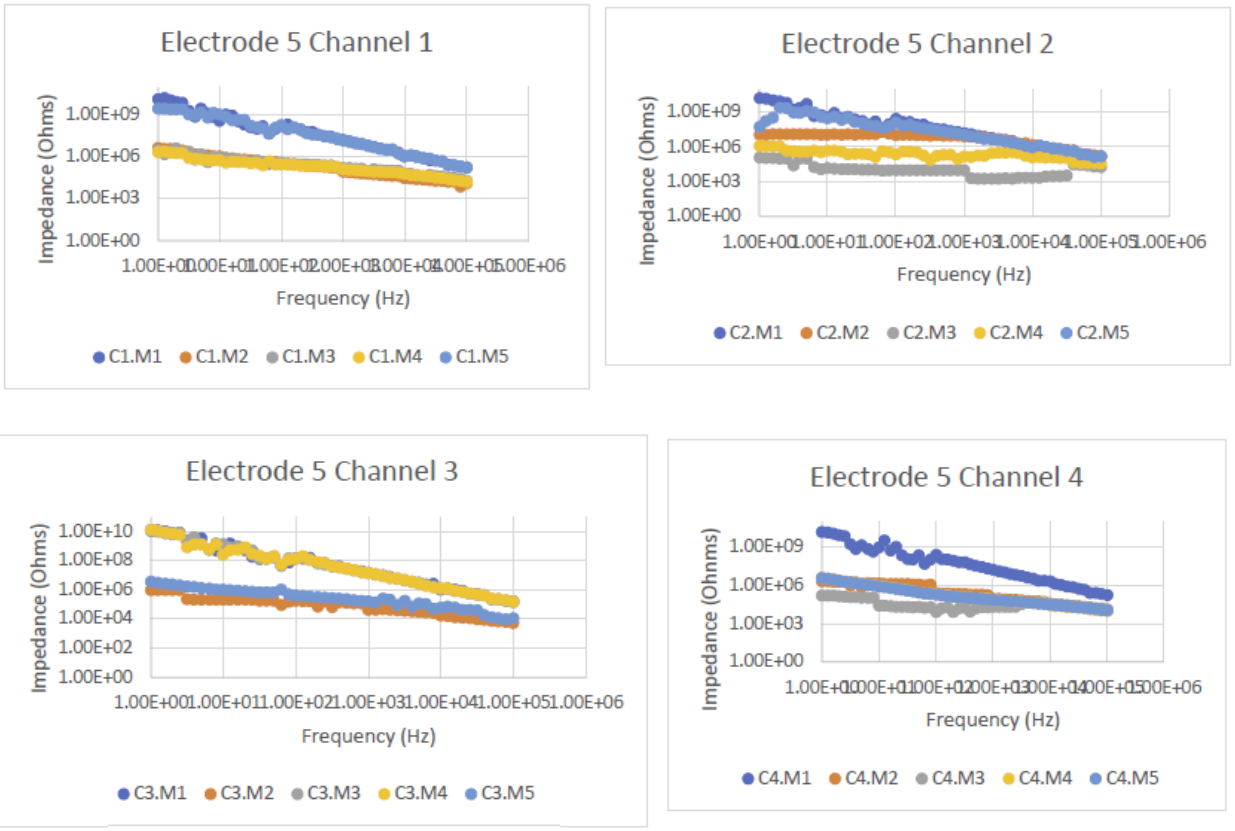

Figure 5.4: Electrode 5

Gray = Measurement 1 at 57°C, Blue = Measurement 2 at 37°C, Red = Measurement 3 at 57°C, Purple = Measurement 4 at 57°C Green = Measurement 5 at 57°C, Brown = Measurement 6 at 57°C
X Axis = Frequency (Hz) Y Axis = Impedance (Ohms)

Box and whisker plots were plotted showing the average impedance values for day 0, day 7, day 14, and day 21 for electrode arrays 1 and 2 (37 °C) as well as the average impedance values for day 0, day 6, day 12, day 18, day 24, and day 30 for electrode arrays 4 and 5 (57°C) at frequencies of 1Hz, 1kHz, and 100 kHz.

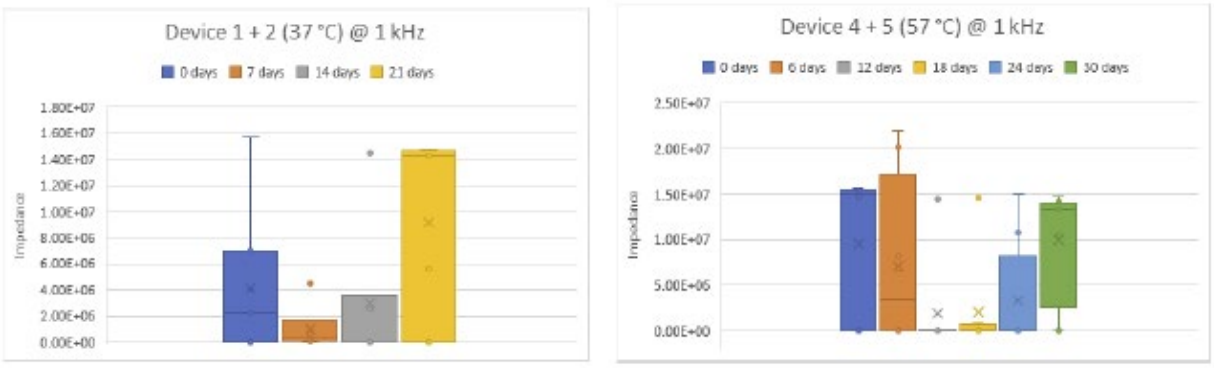

Figure 5.5: Box plot for electrode arrays 1+2 and electrodes 4+5 at 1 kHz

The box plot shows average impedance values for each day EIS was conducted. In addition, the box plots show the distribution of impedance values and any outliers observed within the experiment. Average impedance for electrode arrays 1+2 increased significantly from 4.15E6 at baseline to 9.14E6 ohms at day 21. The average impedance for electrode arrays 4+5 showed a less drastic difference, 9.58E6 to 9.97E6 from baseline measurements to day 30.

Figure 5.6: Box plot for electrode arrays 1+2 and electrodes 4+5 at 1 Hz

Average impedance for electrode arrays 1+2 increased significantly from 2.20E9 at baseline to 9.66E9 ohms at day 21. However, the average impedance from electrode arrays 4+5 decreased from 8.96E9 to 3.55E9 ohms at a frequency of 1 Hz.

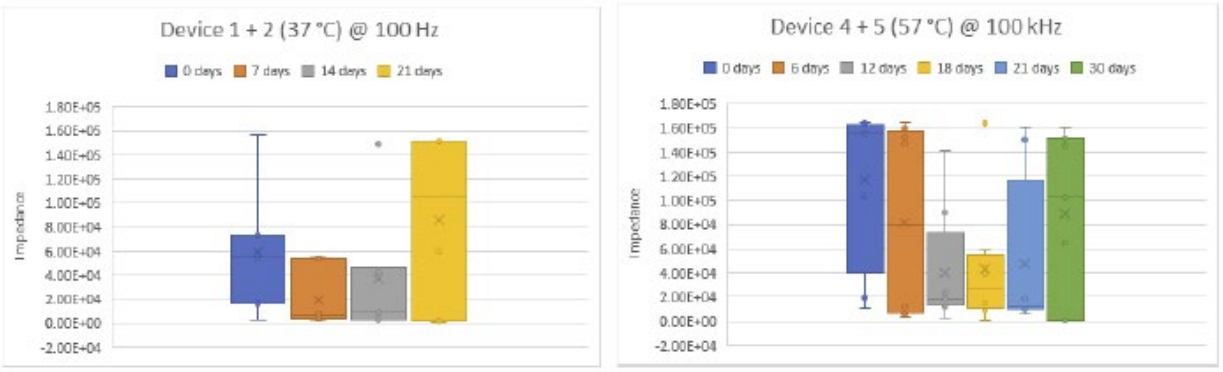

Figure 5.7: Box plot for electrode arrays 1+2 and electrodes 4+5 at 100 kHz

Average impedance for electrode arrays 1+2 increased from 3.93E4 at baseline 8.60E4 ohms at day 21. A higher increase in impedance is seen with electrode array 4+5 aged at 57°C. At baseline the average value was 1.16E5 and by day 21 the impedance decreased drastically to 8.91E4 at a frequency of 100kHz.

While the magnitudes may look similar by just looking at the graphs, in actuality they could be several orders of magnitude off from each other. We cannot just say that the graphs look similar and therefore our hypothesis is valid. Therefore, t-testing was conducted to validate that there is or is not a statistical significance between sets of average impedance values at frequencies of 1 Hz, 1 kHz, and 100 kHz.

The t-testing at 1 kHz (see Table 5.1)was the most useful frequency for us for physiological conditions. We compared the tested two tail P value to our threshold of 0.05. If the P value was below the threshold, then we can reject the null hypothesis. If the two tail P value is above, then we can accept our null hypothesis. P values stayed well above 0.05 at interval day 0 to day 7 and day 7 to day 14. However, we see that when looking at the P values from day 14 to

day 21 we see that the P value drops to 0.09. This is above threshold which tells us that these averages are not statistically significant from each other, but the drastic change in P values going from 0.39 to 0.09 could be from the fact that channel 3 from electrode 2 was removed from the array when testing and PBS solution could have entered into the electrode thus compromising the electrode. Similar observations were noticed in previous research conducted in 1998 by Rousche and Normann. Overall, these electrodes at 1 kHz are robust enough to for at least 30 days of aging in 37°C.

Table 5.1: t–Test Conducted on Electrode Array 1 and 2 Aged in 37°C at 1 kHz

t-Test: Two-Sample Assuming Unequal Variances

	Day 0	*Day 7*
Mean	4150708	1040154
Variance	3.27E+13	2.6E+12
Observatio	7	7
Hypothesiz	0	
df	7	
t Stat	1.38609	
P(T<=t) one	0.104133	
t Critical one	1.894579	
P(T<=t) two	0.208266	
t Critical two	2.364624	

t-Test: Two-Sample Assuming Unequal Variances

	Day 7	*Day 14*
Mean	1040154	2954556
Variance	2.6E+12	2.8E+13
Observatio	7	7
Hypothesiz	0	
df	7	
t Stat	-0.915931	
P(T<=t) one	0.195083	
t Critical one	1.894579	
P(T<=t) two	0.390166	
t Critical two	2.364624	

t-Test: Two-Sample Assuming Unequal Variances

	Day 14	*Day 21*
Mean	2954556	9141963
Variance	2.8E+13	4.97E+13
Observatio	7	7
Hypothesiz	0	
df	11	
t Stat	-1.856883	
P(T<=t) one	0.045143	
t Critical one	1.795885	
P(T<=t) two	0.090287	
t Critical two	2.200985	

t-Test: Two-Sample Assuming Unequal Variances

	Day 0	*Day 21*
Mean	4150708	9141963
Variance	3.27E+13	4.97E+13
Observatio	7	7
Hypothesiz	0	
df	12	
t Stat	-1.454818	
P(T<=t) one	0.085687	
t Critical one	1.782288	
P(T<=t) two	0.171374	
t Critical two	2.178813	

Out of curiosity we conducted t-testing from average impedance values from day 7 to day 21. We wanted to know why the impedance values degreased in the beginning to as low as 1.04E6 then increased beginning from day 14 to day 21.

Table 5.2: t-Test Conducted on Electrode Array 1 and 2 Aged in 37°C at 1 kHz

t-Test: Two-Sample Assuming Unequal Variances		
	Variable 1	*Variable 2*
Mean	1040154.286	9141962.714
Variance	2.60066E+12	4.9743E+13
Observatio	7	7
Hypothesiz	0	
df	7	
t Stat	-2.962776821	
P(T<=t) one	0.010511026	
t Critical one	1.894578605	
P(T<=t) two	0.021022052	
t Critical two	2.364624252	

We see that the P value is 0.02 < 0.05 and the average impedance values do increase from Average impedance at day 7 to day 21. This tells us that the two average values are statistically significant, therefore, we can reject the null hypothesis. Connection could have played a factor into why we see such an increase with impedance values. Also, the 3rd channel was removed during EIS testing causing delamination of the electrode, compromising the electrode array.

Table 5.3: **t-Test Conducted on Electrode Array 4 and 5 Aged in 57°C at 1 kHz**

t-Test: Two-Sample Assuming Unequal Variances		
	Day 0	*Day 6*
Mean	9586831	7153225
Variance	6.21E+13	8.41E+13
Observatio	8	8
Hypothesiz	0	
df	14	
t Stat	0.569241	
P(T<=t) one	0.289106	
t Critical one	1.76131	
P(T<=t) two	0.578212	
t Critical two	2.144787	

t-Test: Two-Sample Assuming Unequal Variances		
	Day 6	Day 12
Mean	7153225	1880485
Variance	8.41E+13	2.55E+13
Observatio	8	8
Hypothesiz	0	
df	11	
t Stat	1.424648	
P(T<=t) one	0.091003	
t Critical one	1.795885	
P(T<=t) two	0.182007	
t Critical two	2.200985	

t-Test: Two-Sample Assuming Unequal Variances

	Day 12	*Day 18*
Mean	1880485	2010529
Variance	2.55E+13	2.6E+13
Observatio	8	8
Hypothesiz	0	
df	14	
t Stat	-0.051257	
P(T<=t) one	0.479922	
t Critical one	1.76131	
P(T<=t) two	0.959845	
t Critical two	2.144787	

t-Test: Two-Sample Assuming Unequal Variances

	Day 18	*Day 24*
Mean	2287713	3275598
Variance	2.96E+13	3.63E+13
Observatio	7	8
Hypothesiz	0	
df	13	
t Stat	-0.333617	
P(T<=t) one	0.371994	
t Critical one	1.770933	
P(T<=t) two	0.743988	
t Critical two	2.160369	

t-Test: Two-Sample Assuming Unequal Variances

	Day 24	*Day 30*
Mean	3275598	9972777
Variance	3.63E+13	3.94E+13
Observatio	8	8
Hypothesiz	0	
df	14	
t Stat	-2.178006	
P(T<=t) one	0.023498	
t Critical one	1.76131	
P(T<=t) two	0.046996	
t Critical two	2.144787	

t-Test: Two-Sample Assuming Unequal Variances

	Day 0	*Day 30*
Mean	9586831	9972777
Variance	6.21E+13	3.94E+13
Observatio	8	8
Hypothesiz	0	
df	13	
t Stat	-0.108365	
P(T<=t) one	0.457681	
t Critical one	1.770933	
P(T<=t) two	0.915361	
t Critical two	2.160369	

The greatest change in average impedance was observed at 57°C for electrodes 4+5 at 1 kHz. After conducting the T test we see that the P values are well above 0.05 for intervals 0 – 6 days, 6 – 12 days, 12 – 18 days, and 18 – 24 days. P values do drop significantly from 0.744 to 0.04 from day 24 to day 30, which is below the threshold. This indicated to us that when conducting accelerated aging on these 4-channel electrode arrays they start to show signs of delamination at a simulated aging period of 240 days. However, the P value from baseline at day 0 to day 30 at 1 kHz was .091 indicating that the average impedance values are not statistically significant from each other. Some factors that could have affected these results could have been the time the electrode was taken out of incubation for EIS measurement. When conducting EIS every channel

was measured individually. The temperature of the electrode could have changed testing channel 1 to channel 4. In addition, there were times when we could conduct EIS for electrodes 4 and 5 and the PBS solution had evaporated leaving half of the electrode array exposed to aging in air for an unknown period of time.

Table 5.4: **t-Test Conducted on Electrode Array 1 and 2 Aged in 37°C at 1 Hz**

t-Test: Two-Sample Assuming Unequal Variances

	Day 0	*Day 7*
Mean	2201940871	11634571.4
Variance	1.40437E+19	4.3909E+14
Observatio	7	7
Hypothesiz	0	
df	6	
t Stat	1.546345622	
P(T<=t) one	0.086490461	
t Critical on	1.943180281	
P(T<=t) two	0.172980921	
t Critical tw	2.446911851	

t-Test: Two-Sample Assuming Unequal Variances

	Day 7	*Day 14*
Mean	11634571.43	3055916657
Variance	4.39086E+14	6.3597E+19
Observatio	7	7
Hypothesiz	0	
df	6	
t Stat	-1.009981887	
P(T<=t) one	0.175742567	
t Critical on	1.943180281	
P(T<=t) two	0.351485134	
t Critical tw	2.446911851	

t-Test: Two-Sample Assuming Unequal Variances

	Day 14	*Day 21*
Mean	3055916657	9667363609
Variance	6.35972E+19	2.2208E+20
Observatio	7	6
Hypothesiz	0	
df	7	
t Stat	-0.973767449	
P(T<=t) one	0.18130617	
t Critical on	1.894578605	
P(T<=t) two	0.362612341	
t Critical tw	2.364624252	

t-Test: Two-Sample Assuming Unequal Variances

	Day 0	*Day 21*
Mean	2201940871	9667363609
Variance	1.40437E+19	2.2208E+20
Observatio	7	6
Hypothesiz	0	
df	6	
t Stat	-1.19513357	
P(T<=t) one	0.138563258	
t Critical on	1.943180281	
P(T<=t) two	0.277126515	
t Critical tw	2.446911851	

For electrode arrays 1 and 2 we see that the average impedance does increase from baseline of 2.20E9 to 9.66E9 at day 21, but the P value is well above 0.05 at 0.27 which would tell us that these averages are not statistically significant from each other. The increase in impedance could indicate a bad connection from the alligator clip to the measured channel. Further studies via scanning electron microscopy could have been conducted for future protocols

to show the surface of the electrode at a microscopic level. We can then see if there is delamination on the surface of the electrode. This would indicate why the impedance increase from baseline to day 21 instead of it being due to a bad connection to the alligator clip during EIS measurement.

Table 5.5: t-Test Conducted on Electrode Array 4 and 5 Aged in 57°C at 1 Hz

t-Test: Two-Sample Assuming Unequal Variances

	Day 0	*Day 6*
Mean	8963769125	1037596825
Variance	5.56339E+19	8.4976E+18
Observatio	8	8
Hypothesiz	0	
df	9	
t Stat	2.799450839	
P(T<=t) one	0.010365613	
t Critical on	1.833112933	
P(T<=t) two	0.020731226	
t Critical two	2.262157163	

t-Test: Two-Sample Assuming Unequal Variances

	Day 6	*Day 12*
Mean	1037596825	1384024538
Variance	8.4976E+18	1.5254E+19
Observatio	8	8
Hypothesiz	0	
df	13	
t Stat	-0.201053019	
P(T<=t) one	0.421884334	
t Critical on	1.770933396	
P(T<=t) two	0.843768669	
t Critical two	2.160368656	

t-Test: Two-Sample Assuming Unequal Variances

	Day 12	*Day 18*
Mean	1384024538	1758869771
Variance	1.52541E+19	2.4665E+19
Observatio	8	8
Hypothesiz	0	
df	13	
t Stat	-0.167806166	
P(T<=t) one	0.434659087	
t Critical on	1.770933396	
P(T<=t) two	0.869318174	
t Critical two	2.160368656	

t-Test: Two-Sample Assuming Unequal Variances

	Day 18	*Day 24*
Mean	1758869771	348506250
Variance	2.46648E+19	9.1154E+17
Observatio	8	8
Hypothesiz	0	
df	8	
t Stat	0.788781787	
P(T<=t) one	0.22648924	
t Critical on	1.859548038	
P(T<=t) two	0.452978479	
t Critical two	2.306004135	

t-Test: Two-Sample Assuming Unequal Variances

	Day 24	*Day 30*
Mean	348506250	3557388617
Variance	9.11537E+17	3.2764E+19
Observatio	8	6
Hypothesiz	0	
df	5	
t Stat	-1.359086422	
P(T<=t) one	0.116103993	
t Critical on	2.015048373	
P(T<=t) two	0.232207986	
t Critical two	2.570581836	

t-Test: Two-Sample Assuming Unequal Variances

	Day 0	*Day 30*
Mean	8963769125	3557388617
Variance	5.56339E+19	3.2764E+19
Observatio	8	6
Hypothesiz	0	
df	12	
t Stat	1.534387926	
P(T<=t) one	0.075434086	
t Critical on	1.782287556	
P(T<=t) two	0.150868172	
t Critical two	2.17881283	

At low frequencies (1 Hz) we see that aging the electrode for a simulated period of 240 days gives us a decrease in impedance with the P value of 0.15. This is consistent with previous research conducted. As the frequency decreases to 1 Hz the impedance increases, but then will plateau or gradually decrease over the following months or years. At day 30 of aging at 57°C is 240 days in real time. This result does reject the null hypothesis that overall impedance should not change as the electrode array is aged for up to 240 days.

Table 5.6: t-Test Conducted on Electrode Array 1 and 2 Aged in 37°C at 100 kHz

t-Test: Two-Sample Assuming Unequal Variances

	Day 0	*Day 7*
Mean	59338.71429	19174.57143
Variance	2469058352	578036434
Observatio	7	7
Hypothesiz	0	
df	9	
t Stat	1.925061202	
P(T<=t) one	0.043176702	
t Critical on	1.833112933	
P(T<=t) two	0.086353403	
t Critical tw	2.262157163	

t-Test: Two-Sample Assuming Unequal Variances

	Day 7	*Day 14*
Mean	19174.57143	36676.42857
Variance	578036434	2802348298
Observatio	7	7
Hypothesiz	0	
df	8	
t Stat	-0.796434545	
P(T<=t) one	0.224383287	
t Critical on	1.859548038	
P(T<=t) two	0.448766575	
t Critical tw	2.306004135	

t-Test: Two-Sample Assuming Unequal Variances

	Day 14	*Day 21*
Mean	36676.42857	86034.6
Variance	2802348298	5574843090
Observatio	7	6
Hypothesiz	0	
df	9	
t Stat	-1.35368873	
P(T<=t) one	0.104425177	
t Critical on	1.833112933	
P(T<=t) two	0.208850353	
t Critical tw	2.262157163	

t-Test: Two-Sample Assuming Unequal Variances

	Day 0	*Day 21*
Mean	59338.71429	86034.6
Variance	2469058352	5574843090
Observatio	7	6
Hypothesiz	0	
df	8	
t Stat	-0.745630226	
P(T<=t) one	0.238612348	
t Critical on	1.859548038	
P(T<=t) two	0.477224696	
t Critical tw	2.306004135	

Table 5.7: t-Test Conducted on Electrode Array 1 and 2 Aged in 57°C at 100 kHz

t-Test: Two-Sample Assuming Unequal Variances

	Day 0	*Day 6*
Mean	116682.5	82134.75
Variance	4.33E+09	6.26E+09
Observatio	8	8
Hypothesiz	0	
df	14	
t Stat	0.949474	
P(T<=t) one	0.179242	
t Critical on	1.76131	
P(T<=t) two	0.358483	
t Critical tw	2.144787	

t-Test: Two-Sample Assuming Unequal Variances

	Day 6	*Day 12*
Mean	82134.75	39922
Variance	6.26E+09	2.38E+09
Observatio	8	8
Hypothesiz	0	
df	12	
t Stat	1.2846	
P(T<=t) one	0.111588	
t Critical on	1.782288	
P(T<=t) two	0.223177	
t Critical tw	2.178813	

t-Test: Two-Sample Assuming Unequal Variances

	Day 12	*Day 18*
Mean	39922	43167.61
Variance	2.38E+09	2.75E+09
Observatio	8	8
Hypothesiz	0	
df	14	
t Stat	-0.128239	
P(T<=t) one	0.449892	
t Critical on	1.76131	
P(T<=t) two	0.899784	
t Critical tw	2.144787	

t-Test: Two-Sample Assuming Unequal Variances

	Day 18	*Day 24*
Mean	43167.61	47499.88
Variance	2.75E+09	4.47E+09
Observatio	8	8
Hypothesiz	0	
df	13	
t Stat	-0.144293	
P(T<=t) one	0.443741	
t Critical on	1.770933	
P(T<=t) two	0.887482	
t Critical tw	2.160369	

t-Test: Two-Sample Assuming Unequal Variances

	Day 24	*Day 30*
Mean	47499.88	89142.09
Variance	4.47E+09	4.76E+09
Observatio	8	7
Hypothesiz	0	
df	13	
t Stat	-1.183331	
P(T<=t) one	0.128933	
t Critical on	1.770933	
P(T<=t) two	0.257866	
t Critical tw	2.160369	

t-Test: Two-Sample Assuming Unequal Variances

	Day 0	*Day 30*
Mean	116682.5	89142.09
Variance	4.33E+09	4.76E+09
Observatio	8	7
Hypothesiz	0	
df	13	
t Stat	0.787956	
P(T<=t) one	0.222427	
t Critical on	1.770933	
P(T<=t) two	0.444853	
t Critical tw	2.160369	

Some other criteria that could have affected the results was that the PBS solution would evaporate in 57 °C , so when coming into measure EIS there were times that the electrode was not

in solution due to evaporation, so the electrode was being aged in air and not solution for an unknown period. When the electrodes were taken out from the incubator not all the channels were measured at once, so that gave the electrode time to cool down in solution.

Initially, this protocol was going to include both EIS measurements and CV, but in the beginning stages we tested on a "dummy" electrode to make sure that we were getting results similar to what Qualia sent us giving us reassurance that the experimental setup is correct. However, we kept getting overload on the electrodes when conducting CV measurements. This resulted in hydrogen gas bubbles forming on the working electrode, which compromised the electrode function. Therefore, in order to preserve the other electrodes for the experiment, CV testing was put on hold. This is shown in Figure 5.8. On the left we have a clean electrode in which all the channels are clearly visible, but once the electrode experienced overload those channels became delaminated as shown in the image on the right. This was a good thing because we know these devices are highly delicate, so when conducting EIS over a period we must be careful when measuring and taking the electrode in and out of the PBS solution.

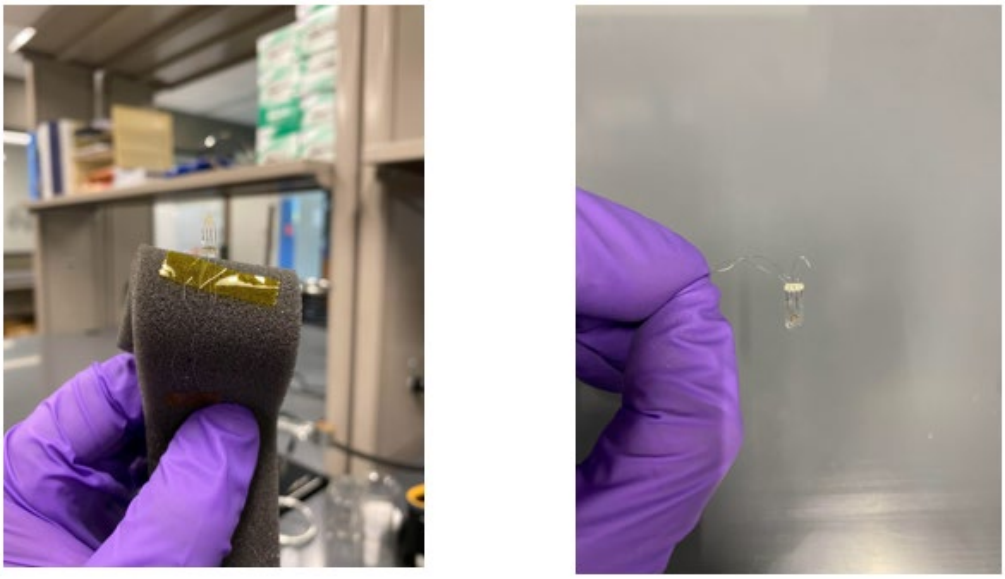

Figure 5.8: Fully intact electrode array (left); delaminated array (right).

CHAPTER 6

CONCLUSION

We have developed a protocol for measuring EIS on commercially fabricated electrodes. Our results indicated that the average impedance does increase with electrodes 1 and 2 at 37°C from day 0 to day 30 for a frequency of 1 kHz. Even though our P values did not go below the threshold they did drop at day 14 to day 21. This could be due to delamination of the electrode. Channel 3 was removed from the electrode array when EIS was conducted. Further SEM testing would help us validate that the surface of the electrode has been changed. The average impedance did increase from day 24 to day 30 for electrodes 4 and 5 for 57°C at 1 kHz. The best frequency for monitoring the implant degradation is the frequency that gives the greatest change in impedance (highest sensitivity). We see from the average impedance values at 1 Hz is the greatest going from 2.2E9 to 9.7E9 Ohms. In addition, cable connection does matter. If there is not a good connection, there are harmonics observed in EIS and when the clips are perpendicular to the electrode wire then that adds capacitance. We did not have a faraday cage for the study, so there could have been added noise from that. These electrode arrays from Qualia were "B" grade, so we understood from the beginning that the electrochemical characteristics might not show stable recordings. Overall, aging electrodes in PBS solution at 37 °C and 57 °C show a change in the impedance, rejecting our hypothesis. Low - high impedance was observed as frequency was high – low. The same trend was also seen in similar protocols conducted in previous research. Future applications of this protocol will be very impactful for Dr. Ecker's lab as they develop their electrodes for GI disorders. Some challenges do remain such as CV testing and acquiring a faraday cage, but this gave extensive insight into electrochemical characteristics of neural electrodes. In addition, we know what to look for when measuring EIS and what not to look for and now

experimental set up for conducting EIS on microelectrodes is very crucial to obtaining accurate results.

APPENDIX A

EIS SET-UP

Test protocol can be accessed directly from:

Experiments - Electrochemical Impedance - Potentiostatic EIS

Settings:

Output File: EIS- [device type]-[YY-MM-DD]- [device # on wafer]- [electrode number] Initial

Frequency (Hz)	100000
Final Frequency (Hz)	1
Points/decard	10
AC Voltage (mV rms)	10
DC Voltage (V)	0
Area (cm^2)	1

Init. Delay: On; Time (s): 10; Stab. (mV/s): 0 Estimated Z (ohms): 1. E+009

Optimize for: Low Noise

APPENDIX B

CV SET-UP

Test protocol can be accessed directly from:

Experiments - Physical Electrochemistry - Cyclic Voltammetry

Settings:

File Name: CV-[device type]-[YY-MM-DD]-[device # on wafer]-[electrode number] Electrode

Area (cm^2)	1
Initial E (V)	0 vs Eoc
Scan Limit 1 (V)	0.8 vs Eref
Scan Limit 2 (V)	-0.6 vs Eref
Final E (V)	0 vs Eoc
Scan Rate (mV/S)	50
Step Size (Mv)	10
Cycles (#)	3
I/E Range Mode	Auto
Max Current (mA)	0.001
IRComp	CI
PF Corr. (ohm)	0
Equil. Time (s)	5

Init. Delay: On; Time (s): 10; Stab. (mV/s): 0

Running the test:

Once the Sequence Wizard has been set up, click <Run Sequence> When User Prompt pops up after testing, select next connector pad Click <OK> to run test on next electrode on device

Repeat for all electrodes on device

Sequences can be saved using the <Save Sequence> option in the Sequence Wizard Use the <Load Sequence> option in Sequence Wizard to run tests using saved test sequences and parameters

APPENDIX C

RAW DATA FROM EIS MEASUREMENTS

Impedance						
E1.C1						
1 Hz	6.89E+09	2.87E+06	2.96E+06	2.43E+09		
1 KHz	7.04E+06	5.70E+04	4.68E+04	1.47E+07		
100 KHz	7.32E+04	4.67E+03	3.47E+03	1.51E+05		
E1.C2						
1 Hz	9.60E+07	5.89E+07	2.31E+08	1.74E+05		
1 KHz	4.01E+06	4.44E+06	3.58E+06	1.20E+03		
100 KHz	5.35E+04	5.53E+04	4.26E+04	4.09E+02		
E1.C3						
1 Hz	1.24E+07	7.63E+06	1.03E+07	3.84E+09		
1 KHz	2.26E+06	1.72E+06	2.49E+06	5.59E+06		
100 KHz	5.80E+04	5.32E+04	4.67E+04	5.95E+04		
E1.C4						
1 Hz	1.26E+05	1.38E+06	2.11E+10			
1 KHz	1.91E+03	4.12E+05	1.45E+07			
100 KHz	1.63E+04	8.45E+03	1.49E+05			
E2.C1						
1 Hz	2.93E+06	3.38E+06	1.75E+05	8.05E+03		
1 KHz	4.79E+04	6.36E+04	1.97E+04	1.85E+04		
100 KHz	2.65E+03	3.43E+03	9.47E+03	2.16E+03		
E2.C2						
1 Hz	3.09E+06	2.16E+06	1.71E+06	3.84E+10		
1 KHz	2.82E+04	2.06E+04	2.69E+04	1.48E+07		

Impedance						
100 KHz	5.50E+04	2.13E+03	3.05E+03	1.52E+05		
E2.C4						
1 Hz	8.41E+09	5.11E+06	4.86E+06	1.34E+10		
1 KHz	1.57E+07	5.68E+05	2.95E+04	1.43E+07		
100 KHz	1.57E+05	7.11E+03	2.70E+03	1.52E+05		
E4.C1						
1 Hz	1.35E+06	1.89E+07	5.75E+06	6.38E+06	5.47E+06	3.85E+07
1 KHz	5.81E+04	2.02E+07	7.59E+04	1.08E+05	9.17E+04	1.42E+07
100 KHz	1.12E+04	1.60E+05	1.26E+04	1.51E+04	1.04E+04	6.46E+04
E4.C2						
1 Hz	4.24E+06	8.25E+09	3.29E+06	2.53E+06	2.25E+06	1.32E+05
1 KHz	7.61E+04	2.19E+07	1.74E+05	2.09E+05	2.92E+04	1.11E+03
100 KHz	1.90E+04	1.65E+05	8.96E+04	4.34E+04	1.20E+04	3.86E+02
E4.C3						
1 Hz	4.56E+06	8.35E+06	7.13E+06	4.81E+06	4.88E+06	1.27E+05
1 KHz	9.05E+04	6.78E+06	2.01E+05	8.05E+05	7.41E+04	1.11E+03
100 KHz	1.03E+05	1.48E+05	2.33E+04	5.89E+04	1.80E+04	3.59E+02
E4.C4						
1 Hz	1.49E+10	3.36E+06	2.96E+06	1.62E+04	4.08E+06	
1 KHz	1.53E+07	5.02E+04	3.80E+04	1.29E+03	3.34E+04	
100 KHz	1.58E+05	3.68E+03	3.04E+03	6.35E+02	5.84E+03	
E5.C1						
1 Hz	1.33E+10	4.10E+06	2.81E+06	2.11E+06	2.71E+09	

Impedance						
1 KHz	1.53E+07	8.29E+04	1.55E+05	1.15E+05	1.49E+07	
100 KHz	1.64E+05	1.22E+04	1.90E+04	1.57E+04	1.61E+05	1.45E+05
E5.C2						
1 Hz	1.58E+10	1.11E+07	1.16E+05	1.17E+06	5.28E+07	1.32E+10
1 KHz	1.47E+07	8.11E+06	9.66E+03	1.56E+05	1.08E+07	1.47E+07
100 KHz	1.56E+05	1.52E+05	1.84E+04	3.90E+04	1.51E+05	1.52E+05
E5.C3						
1 Hz	1.35E+10	9.78E+05	1.11E+10	1.41E+10	3.91E+06	5.53E+06
1 KHz	1.55E+07	4.35E+04	1.44E+07	1.46E+07	1.66E+05	1.33E+07
100 KHz	1.65E+05	5.60E+03	1.41E+05	1.63E+05	1.18E+04	1.60E+05
E5.C4						
1 Hz	1.42E+10	2.04E+06	1.44E+05	3.95E+06	3.65E+06	8.11E+09
1 KHz	1.56E+07	8.52E+04	1.98E+04	7.02E+04	7.02E+04	1.06E+07
100 KHz	1.58E+05	1.18E+04	1.28E+04	9.25E+03	1.08E+04	1.02E+05

REFERENCES

1. Kim, G. H., Kim, K., Lee, E., An, T., Choi, W., Lim, G., & Shin, J. H. (2018). Recent Progress on Microelectrodes in Neural Interfaces. Materials (Basel, Switzerland), 11(10), 1995. https://doi.org/10.3390/ma11101995

2. Gulino M, Kim D, Pané S, Santos SD and Pêgo AP (2019) Tissue Response to Neural Implants: The Use of Model Systems Toward New Design Solutions of Implantable Microelectrodes. Front. Neurosci. 13:689. doi: 10.3389/fnins.2019.00689

3. González-González, M. A., Kanneganti, A., Joshi-Imre, A., Hernandez-Reynoso, A. G., Bendale, G., Modi, R., Ecker, M., Khurram, A., Cogan, S. F., Voit, W. E., & RomeroOrtega, M. I. (2018). Thin Film Multi-Electrode Softening Cuffs for Selective Neuromodulation. Scientific reports, 8(1), 16390. https://doi.org/10.1038/s41598-01834566-6

4. Niparko, J. K., Altschuler, R. A., Wiler, J. A., Xue, X., & Anderson, D. J. (1989). Surgical Implantation and Biocompatibility of Central Nervous System Auditory Prostheses. Annals of Otology, Rhinology & Laryngology, 98(12), 965–970. https://doi.org/10.1177/000348948909801209

5. Robinson D.A. The electrical properties of metal microelectrodes. Proc. IEEE. 1968;56:1065–1071. doi: 10.1109/PROC.1968.6458

6. Thomas C.A., Springer P.A., Loeb G.E., Berwald-Netter Y., Okun L.M. A miniature microelectrode array to monitor the bioelectric activity of cultured cells. Exp. Cell Res. 1972;74:61–66. doi: 10.1016/0014-4827(72)90481-8

7. Torsi L., Magliulo M., Manoli K., Palazzo G. Organic field-effect transistor sensors: A tutorial review. Chem. Soc. Rev. 2013;42:8612–8628. doi: 10.1039/c3cs60127g.

8. Spira M.E., Hai A. Multi-electrode array technologies for neuroscience and cardiology. Nat. Nanotechnol. 2013;8:83–94. doi: 10.1038/nnano.2012.265

9. Cogan S.F. Neural Stimulation and Recording Electrodes. Annu. Rev. Biomed. Eng. 2008;10:275–309. doi: 10.1146/annurev.bioeng.10.061807.160518.

10. Stett A., Egert U., Guenther E., Hofmann F., Meyer T., Nisch W., Haemmerle H. Biological application of microelectrode arrays in drug discovery and basic research. Anal. Bioanal. Chem. 2003;377:486–495. doi: 10.1007/s00216-003-2149-x.

11. Wang D., Zhang Q., Li Y., Wang Y., Zhu J., Zhang S., Zheng X. Long-term decoding stability of local field potentials from silicon arrays in primate motor cortex during a 2D center out task. J. Neural Eng. 2014;11:036009. doi: 10.1088/1741-2560/11/3/036009.

12. Campbell P.K., Jones K.E., Huber R.J., Horch K.W., Normann R.A. A silicon-based, threedimensional neural interface: Manufacturing processes for an intracortical electrode array. IEEE Trans. Biomed. Eng. 1991;38:758–768. doi: 10.1109/10.83588

13. Scholten, K., & Meng, E. (2015, September 15). Materials for microfabricated implantable devices: A review. Retrieved March 23, 2021, from https://pubs.rsc.org/en/content/articlelanding/2015/LC/C5LC00809C#!divAbstract

14. Kim D.-H., Wiler J.A., Anderson D.J., Kipke D.R., Martin D.C. Conducting polymers on hydrogel-coated neural electrode provide sensitive neural recordings in auditory cortex. Acta Biomater. 2010;6:57–62. doi: 10.1016/j.actbio.2009.07.034

15. Ware, T., Simon, D., Arreaga-Salas, D., Reeder, J., Rennaker, R., Keefer, E., & Voit, W. (2012, May 02). Fabrication of responsive, softening neural interfaces. Retrieved March 23, 2021, from https://onlinelibrary.wiley.com/doi/abs/10.1002/adfm.201200200

16. Patan, M., Shah, T. & Sahin, M. Charge injection capacity of TiN electrodes for an extended voltage range. IEEE Engineering in Medicine and Biology Society. 1, 890– 892, https://doi.org/10.1109/IEMBS.2006.260088 (2006).

17. Weiland, J. D., Anderson, D. J., & Humayun, M. S. (2002). In vitro electrical properties for iridium oxide versus titanium nitride stimulating electrodes. IEEE transactions on biomedical engineering, 49(12 Pt 2), 1574–1579. https://doi.org/10.1109/TBME.2002.805487

18. Schaldach, M., Hubmann, M., Weikl, A., & Hardt, R. (1990). Sputter-deposited TiN electrode coatings for superior sensing and pacing performance. Pacing and clinical electrophysiology : PACE, 13(12 Pt 2), 1891–1895. https://doi.org/10.1111/j.15408159.1990.tb06911.x

19. Biomedical, E. (2008, July). Electrode Characterization and Long - term In Vitro Testing. Retrieved March 31, 2021, from http://www.eiclabs.com/EICBiomedical/DS062008A1EvaluationandTestingJuly2008.pdf

20. Venkatraman, S., Hendricks, J., King, Z. A., Sereno, A. J., Richardson-Burns, S., Martin, D., & Carmena, J. M. (2011). In vitro and in vivo evaluation of PEDOT microelectrodes for neural stimulation and recording. IEEE transactions on neural systems and rehabilitation engineering : a publication of the IEEE Engineering in Medicine and Biology Society, 19(3), 307–316. https://doi.org/10.1109/TNSRE.2011.2109399

21. Longstreath, G. F., Thompson, W. G., Chey, W. D., Houghton, L. A., Mearin, F., & Spiller, R. C. (n.d.). DEFINE_ME. https://www.gastrojournal.org/article/S0016-5085(06)005129/fulltext#section-a8e3cf85-9a4f-4bb2-bf45-4b7cef04bc50.

22. Rakhilin, N., Barth, B., Choi, J. *et al.* Simultaneous optical and electrical *in vivo* analysis of the enteric nervous system. *Nat Commun* **7,** 11800 (2016). https://doi.org/10.1038/ncomms11800

23. Barth, B. B., Huang, H. I., Hammer, G. E., & Shen, X. (2018). Opportunities and Challenges for Single-Unit Recordings from Enteric Neurons in Awake Animals. *Micromachines*, *9*(9), 428. https://doi.org/10.3390/mi9090428

24. Bérces Z., Tóth K., Márton G., Pál I., Kováts-Megyesi B., Fekete Z., Ulbert I., Pongrácz A. Neurobiochemical changes in the vicinity of a nanostructured neural implant. *Sci. Rep.* 2016;6 doi: 10.1038/srep35944

25. Humphrey DR, Schmidt EM. Extracellular single-unit recording methods. In: Boulton AA, et al., editors. *Neurophysiological Techniques.* New York: Humana; 1990. pp. 1–6